RAVEN Performance Modeling

Meguru Ito[1a], Kate Jackson[1], David Andersen[2], Celia Blain[1], and RAVEN team[1,2]

[1] Adaptive Optics Laboratory, Mechanical Engineering Department, University of Victoria, 3800 Finnerty Road, Victoria, British Columbia V8W 3P6, Canada
[2] NRC Herzberg Institute of Astrophysics, 5071 West Saanich Road, Victoria, British Columbia V9E 2E7, Canada

Abstract. Raven is a MOAO demonstrator that will be mounted on the Nasmyth platform of the Subaru telescope and is intended to serve as a pathfinder for future ELT MOAO instruments. We present the Raven wavefront error budget that was used to define the AO architecture. In particular, we focus here on recent simulations of Raven performance for real science targets, and performance as a function of zenith angle. We show that Raven should deliver ≥ 30 % ensquared energy in a 140 mas slit under median conditions.

1 Introduction

Raven will be the first multi-object adaptive optics (MOAO) instrument on an 8 m class telescope feeding a science instrument, IRCS (Infrared Camera and Spectrograph) [1]. MOAO is considered to be important for future extremely large telescope (ELT) because MOAO can make the corrected field wider than single conjugate AO or even Multi-Conjugate AO (MCAO) systems. Raven has an important role as a pathfinder for future MOAO instruments. Raven is expected to not only be a technical demonstrator of MOAO but also a scientific instrument that will push the astronomical frontier. Raven shares many similarities with Canary [2], but Raven will be mounted on a larger telescope, Subaru Telescope. The 8 m aperture of the Subaru Telescope enables science that is unachievable on a 4 m class telescope, and we can access the proven imager and spectrograph IRCS that has been designed to be fed by an AO system.

Raven must feature at least 3 natural guide star (NGS) wavefront sensors (WFSs) and 2 science arms patrolling a 3.5' diameter field of regard (FoR) [3]. An on-axis laser guide star (LGS) WFS will enhance the performance and sky coverage of Raven. Figure 1 shows the functional block diagram of Raven. The three open-loop WFS and two closed loop WFS can be operated either in closed-loop or in open-loop mode. One of the significant features of Raven is 2 science channel each fed by a deployable science pick-off mirror. Two science pick-offs arms will relay the incoming light from 2 science targets. The pick-off moving mechanism must keep the position, the size and the orientation of the pupil unchanged relative to the WFS lenslet arrays.

Future MOAO instruments are required to concentrate a relatively high fraction of the light from a point source in a small spatial pixel, or "spaxel". If a MOAO system does not achieve a high ensquared energy, the multiplexing advantage is severely limited. To achieve a multiplex advantage over AO188 observing one target, Raven is required to deliver 30% ensquared energy in the H-band with three NGSs within a 140 mas slit. Raven should achieve ~40% ensquared energy if the LGS is used as well, assuming median image quality.

In this proceeding, we present the performance modeling of the baseline Raven MOAO system. More details of Raven performance modeling can be found here[4]. It is necessary to determine if Raven can realistically meet the proposed performance requirements and deliver useful MOAO-corrected images to the Subaru IRCS spectrograph. We used MAOS and OOMAO as simulation tools to undertake the simulation. MAOS (Multi-threaded Adaptive Optics Simulator) is a C++ AO simulation tool developed by Lianqi Wang and TMT (Thirty meter telescope) group. OOMAO (Object Oriented Matlab Adaptive Optics) modeling library is a library of Matlab classes developed by Rodolphe Conan for the purpose of facilitating a clear, accessible end to end model.

[a] itomg@uvic.ca

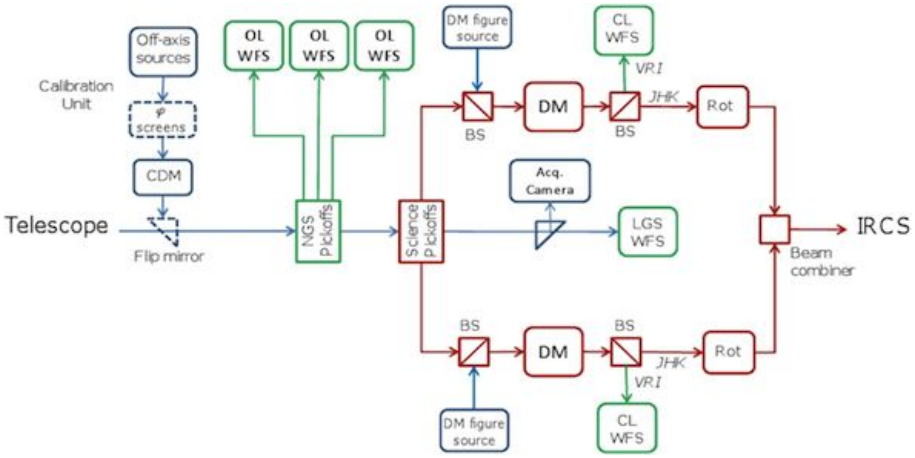

Fig. 1. Functional block diagram of Raven.

2 Baseline Performance

We describe the performance metrics used to evaluate the performance. Since the majority of Raven science will be performed using the spectrograph, ensquared energy within the slit is the most important performance metric. The IRCS echelle slit width is 0.14 arcsecond wide, so we used ensquared energy within 0.14 arcseconds at a wavelength of 1.65 microns (H-band) as the primary performance metric. Since 140 mas is significantly wider than the 42 mas diffraction-limited spot at 1.65 microns, it is clear that Raven performance is most dependent on high spatial order wavefront errors (WFE) and is relatively immune to modest errors at low spatial frequencies including tip/tilt and focus. Therefore another useful metric to evaluate in the simulations is the tip-tilt removed wavefront error. We also calculate Strehl ratio in the H-band and the total WFE.

At this stage of development, we have focused on setting the basic system parameters, such as system order, field of regard, and the limiting magnitude. To understand how performance varies with these and other parameters, we decided to define an asterism with 3 NGS on a ring of 45 arcseconds radius, and then to evaluate the performance at multiple field points within that circle. Figure 2 shows the positions in field at which the performance was measured. We define the average performance over points out to 30 arcseconds from the field center.

The image quality at Subaru Telescope has been measured over a period of years. We had access to the seeing measured between 2000 and 2004. We used the Subaru 50% image quality profile that defined Fried parameter, r_0, is 15.6 cm and outer scale is 30 m. The layers were sampled on a 1/64 m grid. The 3 NGS WFS were on a 45 arcsecond radius ring and have 10 subapertures across the pupil. Selected configuration parameters for the baseline design are given in Table 1.

Table 1. Baseline properties

Telescope diameter		Wavefront sensor	
Outer	8 m	N_{NGS}	3
Inner	2 m	Asterism radius	45 arcsec
Atmosphere		Order	10×10
r_0	15.6 cm	θ_{pix}	0.4 arcsec
L_0	30m	N_{pix}	15
Profile	Subaru 50 %	f_{sample}	500 Hz
Wind_{GL}	5.6 m/s	λ_{WFS}	0.7 μm
Wind_{8km}	19.1 m/s	Deformable mirror	
Wind_{dir}	random	Order	11×11
Sampling	1/64 m	Stroke	infinite

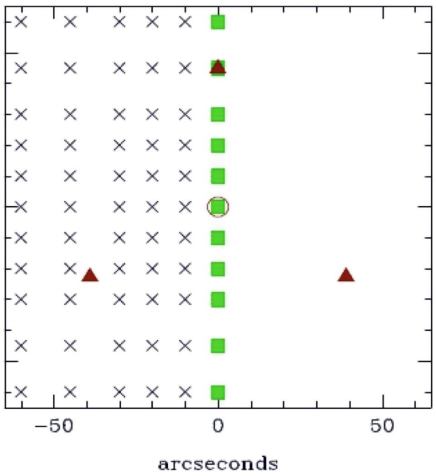

Fig. 2. The geometry of the Raven MAOS simulations. Red triangles show the location of the NGSs. The central red circle shows the LGS field location. H-band PSFs were generated at the locations of the square green points. We measured the Strehl ratio and ensquared energy from these PSFs.

We ran simulations of Raven over 5 seconds (2500 steps at 500 Hz) using the physical optics modeling of the WFS and centroids calculated using the matched filter algorithm, but with no read or photon noise. These simulations show the best performance possible from Raven for bright NGSs (Figure 3. Note the dips in WFE at the radius of the NGS. This dip (with a tip-tilt removed WFE of 180 nm) is consistent with the fitting error for a 11 × 11 order deformable mirror (DM) with a r_0 of 15.6 cm (145 nm). The fact that the performance over most of the field is substantially higher than this ($\sim$ 270 nm) is telling us that the tomographic error is the dominant error source for Raven. This large tomographic error has allowed us to adopt a relatively low order WFS (the 0.8 m d_0 value is quite large for most AO systems) with the possibility of also choosing coarse pixel sampling which will allow us to maintain good corrections for a relatively faint NGS. This system should exceed the Raven 30% ensquared energy requirement.

The performance of the OOMAO model using the baseline parameters is in excellent agreement with the MAOS simulation. Both simulation tools predicted a mean Strehl ratio of 30% for the points within 30 arcseconds of the field center. The two simulations also predicted an identical 43% ensquared energy in this area (when neglecting WFS noise and implementation errors discussed in next section).

3 Error Budget

While the most important figure of merit for Raven is ensquared energy within a 140 mas slit, it is difficult to disentangle how potential sources of WFEs affect this metric. To give a sense of Raven performance, a WFE budget has been built in which it is easier to add together in quadrature the expected contribution of different errors. The high order WFEs are of primary concern, because low order errors (e.g., tip, tilt and focus errors) will broaden the core of the PSF not lead to significant losses in ensquared energy within a 140 mas spaxel. The Raven WFE budget is listed in Table 2. The terms that are included in the simulations below are described, and then some additional implementation errors are listed; these include errors derived from lab tests of an ALPAO DM similar to the Raven science DMs. Simulations used 3 NGS with m_R=14 and a sampling frequency of 180 Hz using the geometry described above. Performance naturally improves with brighter guide stars.

Tomographic error is the dominant error term for Raven operating with just 3 NGSs. If the Subaru LGS is positioned at the center of the field, this error reduced to 105 nm from 175 nm for only 3 NGSs. A certain fraction of this WFE is relatively low order, and will not substantially decrease the ensquared energy.

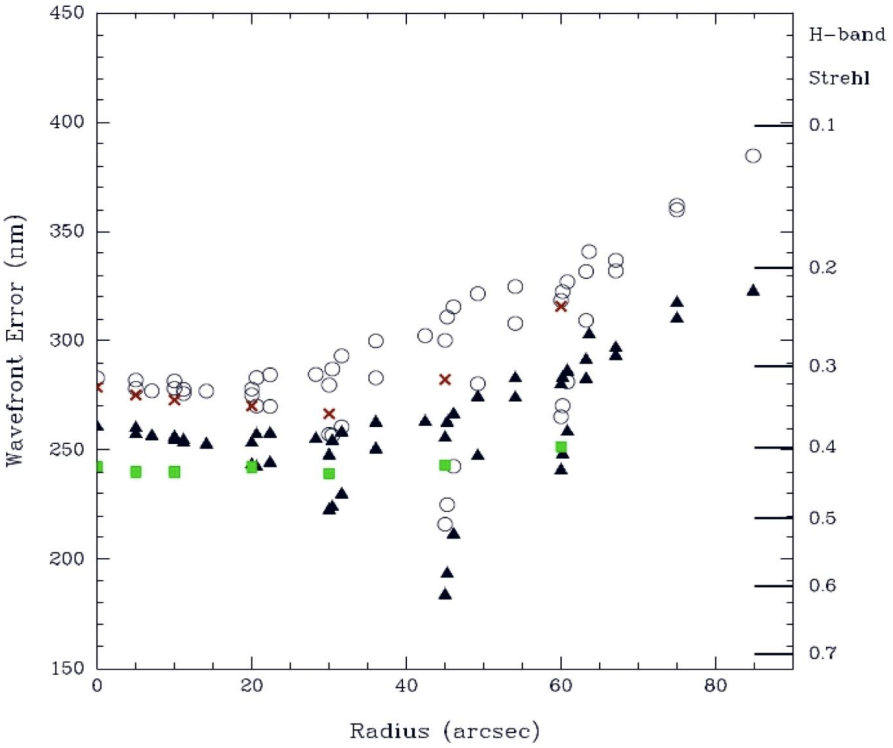

Fig. 3. Raven performance for the baseline NGS-only configuration. Wavefront errors (all modes: open circles; tip-tilt removed: filled triangles) versus radius for the evaluation points shown in Figure 2 for 3 NGS on a 45 arcsecond radius ring. Fractional ensquared energy (within 140 mas; green squares) and Strehl ratios (red x's) measured from the point spread functions (PSFs) are show with the scale on the right (scaled to WFEs by the Maréchal approximation, SR $\approx exp(-\omega^2)$ where ω is the wavefront error in radius.

The 11×11 Raven DM can not be used to fit high order modes and will therefore contribute fitting error term, equal to roughly $\sigma^2_{fit} \approx 0.25(d_0/r_0)^{5/3}$, where d_0 is the inter-actuator spacing projected onto the primary mirror (0.8 m for the baseline system). The large size of the subapertures on the WFS will also contribute an aliasing error that arises from high spatial frequency disturbances that affect the WFS signal. We find from simulations that this error can be characterized by $\sigma^2_{alias} \approx 0.1(d_0/r_0)^{5/3}$, or $\sim$ 100 nm rms WFE due to aliasing in the baseline system.

The WFS noise was calculated from simulations with and without detector noise, photon noise, and sky background. This term obviously depends on guide star magnitude and the sampling rate.

Implementation errors includes calibration error for an open-loop system, the error caused by DM's non-linearities as measured from the ALPAO DM, and the uncorrectable errors on Raven optics. These error sources are not included in the simulations.

In this Raven performance budget, it was found that the implementation errors will further reduce the ensquared energy by $\sim$ 15%. Most of this is due to the open loop calibration error. If a better calibration can be achieved, the implementation error would reduce the ensquared energy by just 10%. As long as no substantial implementation error remains unaccounted, the performance requirement of delivering 30% ensquared energy to the 140 mas spaxel will be met at zenith under median conditions.

Table 2. Raven Wavefront Error Budget (nm RMS)

Term	3 NGS	+ LGS
WFEs from simulation		
Tomography (T/T removed)	175	105
Fitting / Aliasing	200	195
WFS noise	95	95
Total Simulated WFE	280	240
Implementation Errors		
Calibration	90	90
DM non-linearities	35	35
Uncorrectable optical errors	50	50
Implementation Total WFE	110	110
Total WFE	300	265
Total ensquared energy	33 %	33 %

4 Zenith Angle Dependency

MOAO performance will of course depend on the zenith angle of the science target. The distance from the each of the atmospheric layers to the telescope is stretched by the airmass (AM), which is equivalent to AM≡ sec(γ), and the Fried parameter, r_0 is proportional to sec(γ)$^{-3/5}$, where γ is the zenith angle. For the LGS, the distance of the generated beacon and the thickness of the sodium layer are also proportional to sec(γ). As a result, the LGS dims in proportion to cos(γ). The LGS WFS spots will also suffer from increased spot elongation, but this is a second order effect when considering Subaru's centrally launched laser.

Figure 4 shows the wavefront error and Strehl ratio at the center of the FoR for the baseline Raven configuration without the central LGS as a function of airmass. the derived WFEs increase rapidly, and are well-fit by a power-law. Even though the best-fit exponent for a power-law function was greater. One can understand this by considering the overlapping footprints of the guide stars in the meta-pupils corresponding to different atmospheric layers as the zenith angle changes. As the zenith angle increases, the layers essentially get further from the telescope, and the metapupils of the guide stars separate leaving a larger portion of the metapupil for a given layer less well-sampled or even unsensed. If one looks at the power law index as a function of distance from the nearest guide star, this effect becomes clear (Figure 5).

For classical AO systems dominated by fitting error, the WFE should be proportional to AM$^{1/2}$. Since a large fraction of the Raven WFE budget is dominated by tomographic error, we expect that the power law index, β defined from the relation WFE $\propto$ AM$^{\beta}$ will vary with distance from the guide stars (Figure 5). We see that near the NGSs, the $\beta \sim 0.5$, but that β rises to ~ 1 away from the NGSs. The power law index β is large even very close the LGS, because atmospheric turbulence is dominated by tip/tilt which is un-sensible by the LGS WFS. If tip/tilt is excluded, the relation is virtually indistinguishable between LGSs and NGSs.

5 On-Sky Performance

We have completed the initial performance modeling for the Raven baseline system. However, we have to confirm the performance of Raven for real configurations of NGSs presented by real scientific fields. In practice, it is difficult to find three bright NGSs all within a radius of 45 arcsecond and distributed reasonably. We selected a Raven science field and evaluated the performance. The selected example field was a part of open cluster, NGC2301, that is in the Monoceros (Figure 6). The coordinate of field center is R.A.=06:51:37.78, and Dec.=+00:27:27.9. The objects in the white circles of Figure 6 are all stars and we used them as NGSs. The brightness of the NGSs in the R-band are 11.0, 11.1, and 11.5. The red circles show the virtual science targets. We called the stars with the H-band magnitude of 10.2 and 10.6 target 1 and target 2, respectively. The target stars are bright enough for the high-resolution

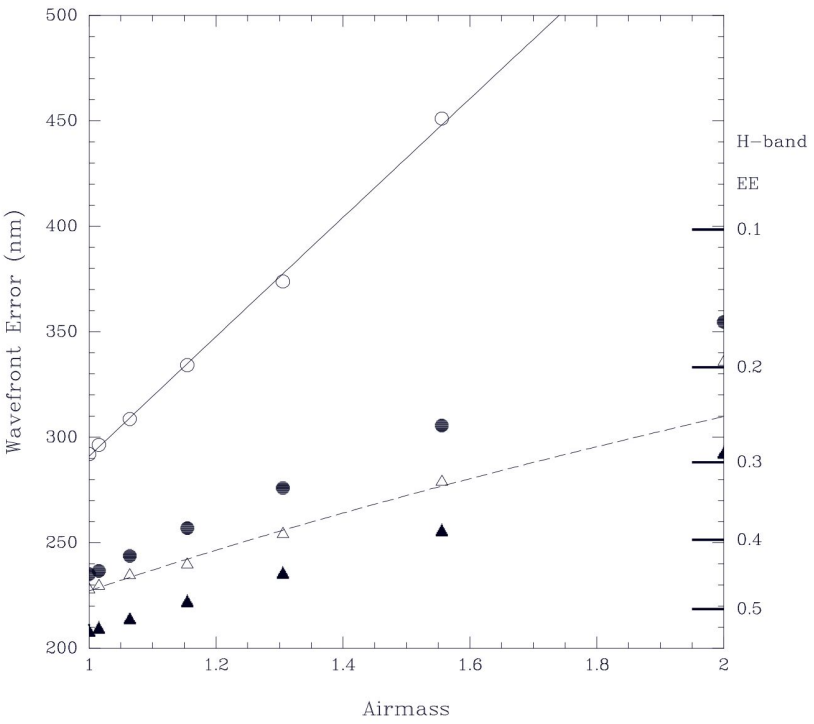

Fig. 4. Wavefront error (open points; scale on left) and H-band ensquared energy (filled points; scale on right) as a function of airmass for a point near a NGS (triangles) and 45 arcseconds from the nearest NGS (circles). The performance drops more rapidly for points in the field far from NGSs. At the location of a NGS, the WFE decrease as $AM^{1/2}$.

spectrograph with narrow slit width in the infrared wavelength. The distances from the field center to each NGS are ~ 60 arcsecond. That is close to the asterism of the baseline system.

We ran MAOS simulations using the configuration of the example field (locations and brightnesses of NGSs). The performance variations with hour angle (i.e. changing zenith angle) were also simulated (Figure 7). The hour angle is derived by the equation, $\cos\gamma = \cos(d + l) - \cos l \cdot \cos d \cdot (1 - \cos h)$, where the h is the hour angle, d is the declination of the field, and l is the latitude of the observer. Consequently, the zenith angle is 19.4° for this example field when the hour angle is zero.

Figure 7 shows the result that the derived ensquared energy for both science targets exceed 35% when the hour angle is close to zero (excluding un-modelable implementation errors described above). The ensquared energy remains greater than 30% until the hour angle reaches 2 hr, corresponding to a zenith angle of ~ 40°.. Raven should meet the requirement of 30% ensquared energy at the zenith if we can find appropriate NGSs.

6 Summary

A baseline MOAO system architecture for Raven has been established and the expected performance of such a system has been simulated using two independent modeling tools, MAOS and OOMAO.

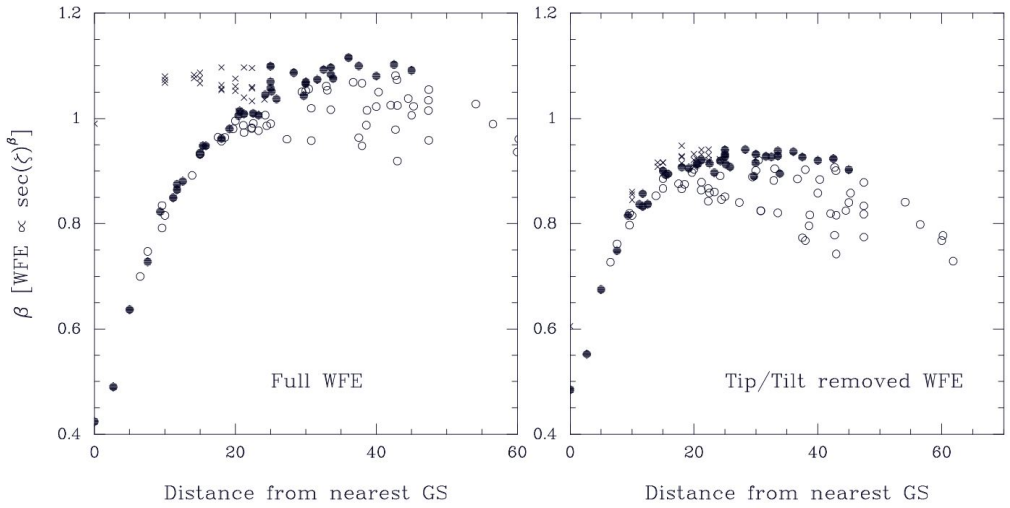

Fig. 5. The power law index β, as defined in the relation WFE $\propto \sec\gamma^{\beta}$, versus distance to the nearest guide star considering the full WFE (left panel) and WFE with the tip/tilt component removed (right panel). Points are labeled by whether the closest guide star is the LGS (x), points are inside the 45 arcsecond diameter ring on which the NGS sit (filled circles) or are outside that ring (open circles).

These two independently-developed AO simulation tools give excellent agreement for the expected performance of Raven. Based on these results, it has been established that Raven should be able to meet the design requirement that 30 % ensquared energy be delivered within a 140 mas wide IRCS slit if three NGS are used, and performance will improve dramatically if the single Subaru facility on-axis LGS WFS is also included (up to ~ 40 % ensquared energy in median conditions). Employing one LGS beacon also greatly improves the sky coverage because Raven can operate with 3 NGSs that are $m_R < 14.5$ and perhaps even fainter.

We found that the degradation of performance with zenith angle is dependent on the distance to the nearest guide star; performance degrades more rapidly the further away from a guide star the science object sits.

Raven performance for real science targets has also simulated and it showed good ensquared energy of > 35 % at the smallest zenith angle with three bright NGSs ($m_R \sim 11$). As these results, Raven will meet the requirement of 30 % ensquared energy at the zenith in the average atmospheric condition.

References

1. Kobayashi, N., et al. Proc. SPIE 4008 (2000)
2. Gendron, E., et al. A&A, 529L (2011)
3. Conan, R., et al. Proc. SPIE 7736 (2010)
4. Andersen, D., et al. *accepted by PASP*, (2012)

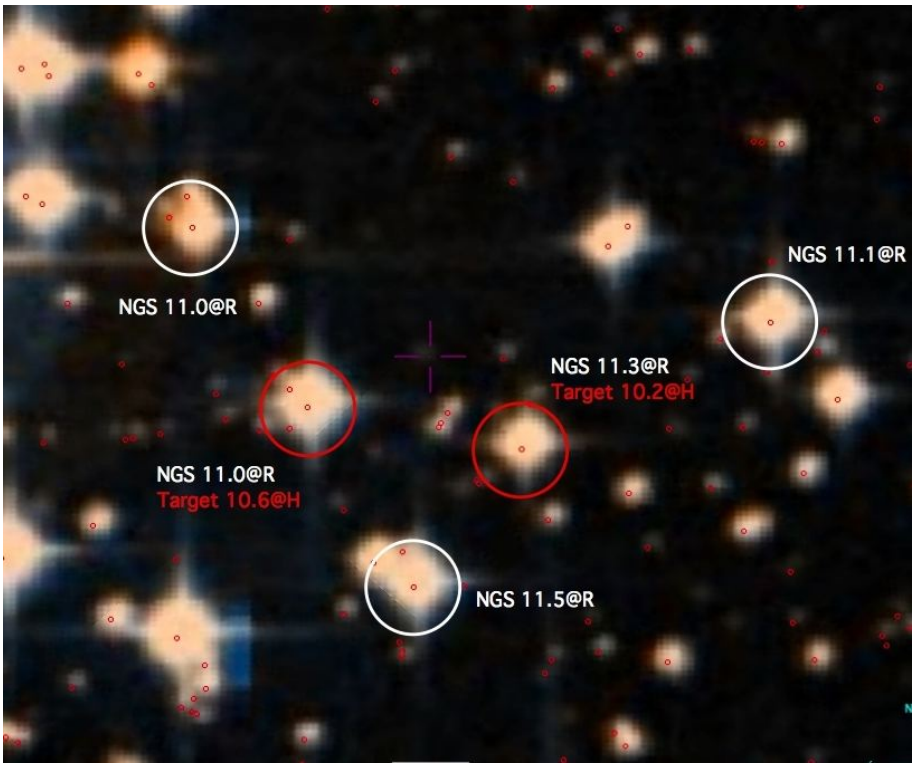

Fig. 6. Digitized Sky Survey (DSS) colored image of example field in NGC2301. NGC2301 is an open cluster in the Monoceros. The coordinate of field center (purple cross) is R.A. = 06:51:37.78, Dec. = +00:27:27.9. The white circles and red circles describe NGSs and virtual science targets, respectively. North is to the top and east to the left.

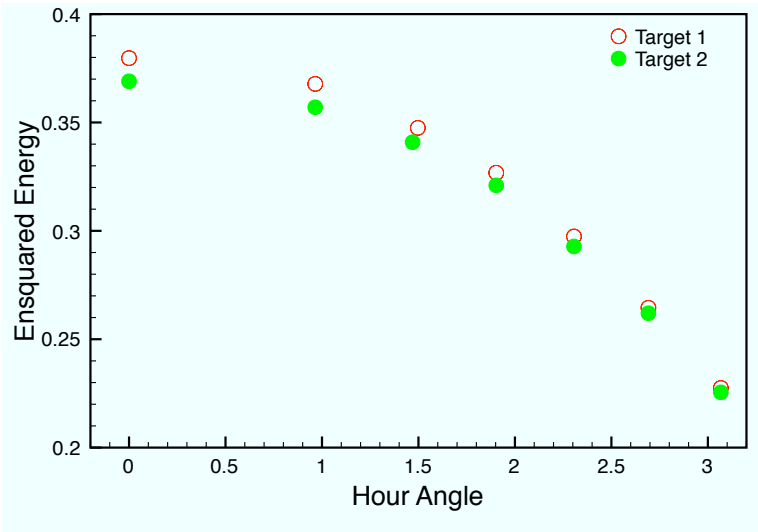

Fig. 7. The ensquared energy of both target versus hour angle. Target 1 (open red circles) and 2 (filled green circles) correspond to the star with the H-band magnitude of 10.2 and 10.6, respectively. The hour angle is equivalent to the zenith angle of the target field. In this case, the hour angle of zero is equal to the zenith angle of 19.4°.